Supplementary information

Single-Layer ReS_2: Two-Dimensional Semiconductor with Tunable In-Plane Anisotropy

Yung-Chang Lin[1*], Hannu-Pekka Komsa[2], Chao-Hui Yeh[3], Torbjörn Björkman[2,4], Zheng-Yong Liang [2], Ching-Hwa Ho[5], Ying-Sheng Huang[6], Po-Wen Chiu[3], Arkady V. Krasheninnikov[7,8], and Kazu Suenaga[1*]

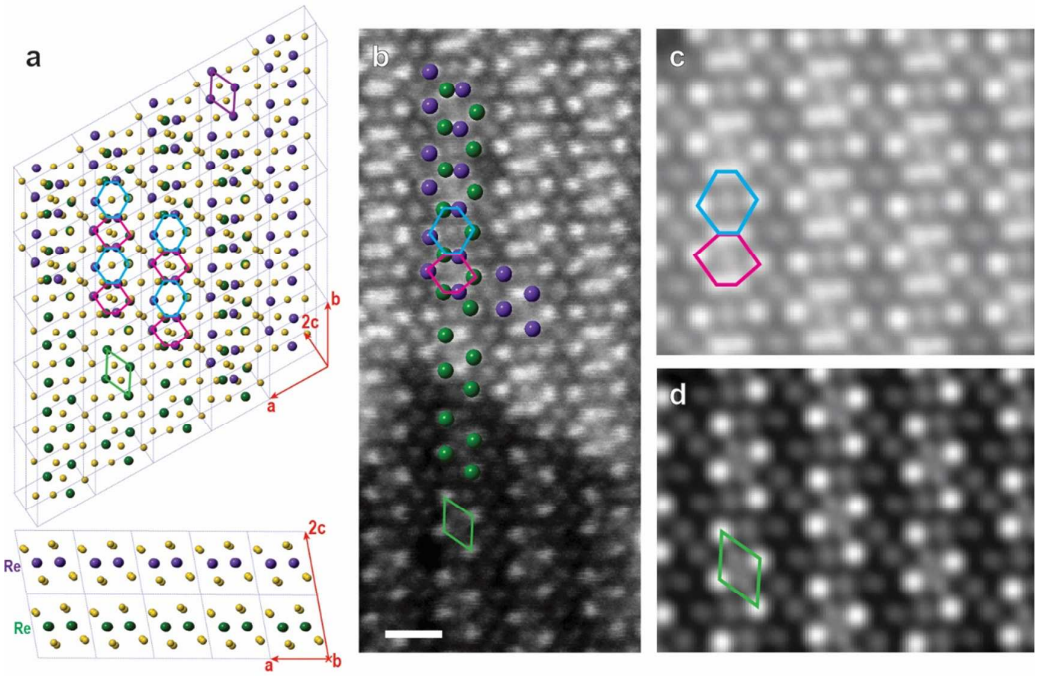

Supplementary Figure S1. (a) The atomic structure of bilayer $ReSe_2$ in basal plane and cross-section view. The Re atoms in two distinct layers are presented by green and purple sphere, respectively. The c-axis of $ReSe_2$ is tilt in an angle resulting in unconventional stacking that Re atoms (green atoms) are not overlapped with the atoms in another layers (purple atoms). (b) The ADF image of single-layer and bilayer $ReSe_2$. The bilayer $ReSe_2$ shows distorted hexagonal structure (blue and pink hexagons). (c,d) The STEM simulation images of bilayer and single-layer $ReSe_2$, respectively. The image simulations were performed using QSTEM. Scale bar is 0.5 nm.

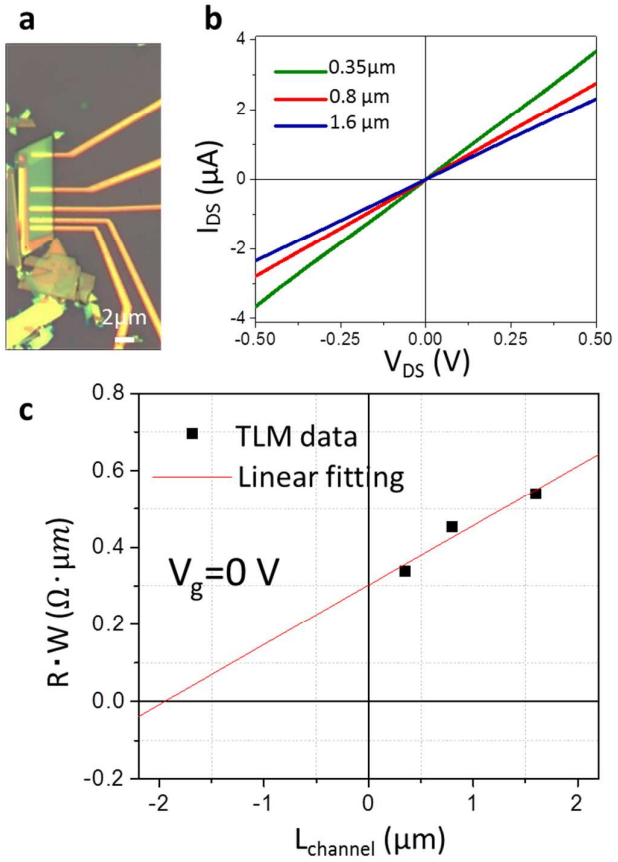

Supplementary Figure S2. (a) An optical image of four-probe transmission line method (TLM) measurement on spared ReS_2 flake. Scale bar is 1 μm. (b) The I-V characteristic of ReS_2 in distinct channel length. (c) The contact resistance Rc = 60.41 kΩ which is extracted from the TLM.

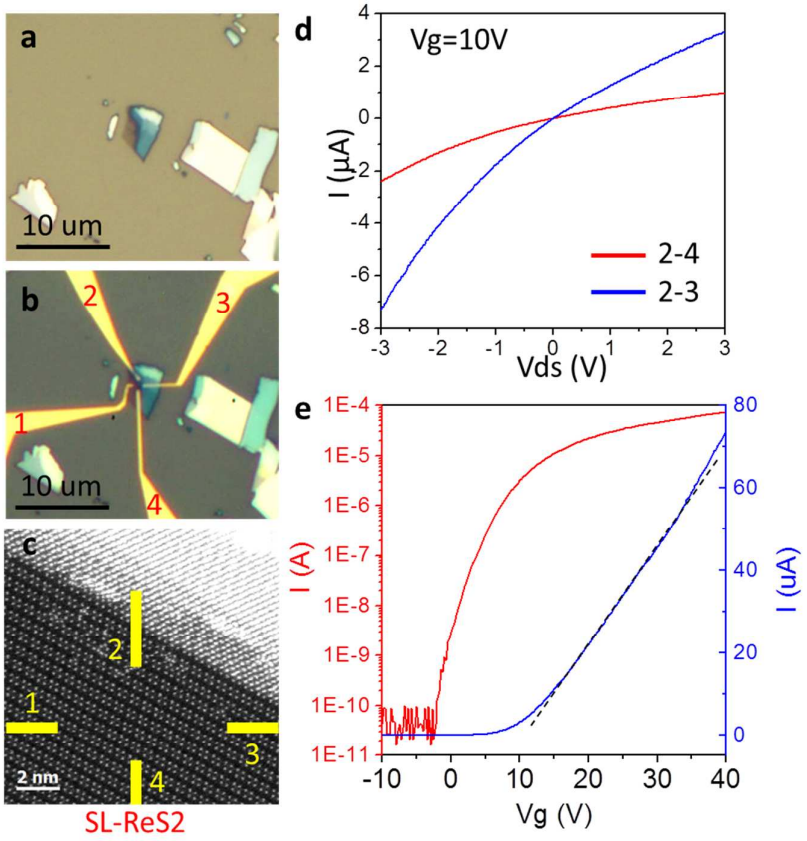

Supplementary Figure S3. The optical microscope images of (a) an exfoliated ReS_2 flake on SiO_2/Si substrate and (b) Four contacts are deposited on the single layer region. (c) An ADF image of the single layer ReS_2. (d) The direction-dependent I-V characteristics with applied back gate voltage Vg=10V. The two-terminal conductance parallel and perpendicular to the DS-chains are G_{24}=2.43 μS and G_{23}=0.8 μS for Vds=-3V and Vg=10V. (e) The transfer characteristic with drain-source bias of -3V between probes 2-4. The field effect mobility is 69.3 cm^2/Vs.

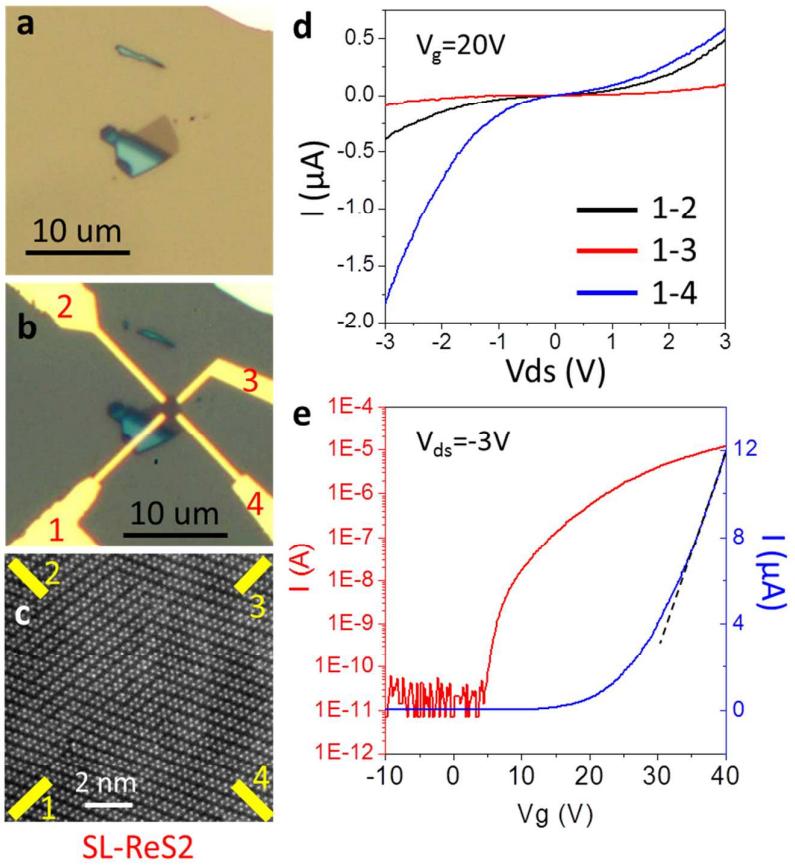

Supplementary Figure S4. The optical microscope images of (a) an exfoliated ReS_2 flake on SiO_2/Si substrate and (b) Four contacts are deposited on the single layer region. (c) An ADF image of the single layer ReS_2. (d) The direction-dependent I-V characteristics with applied back gate voltage Vg=20V. The two-terminal conductance along different direction G_{14}=0.61 μS, G_{12}=0.129 μS and G_{13}=0.028 μS for Vds=-3V and Vg=20V. (e) The transfer characteristic with drain-source bias of -3V between probes 1-4. The field effect mobility is 18.7 cm^2/Vs.

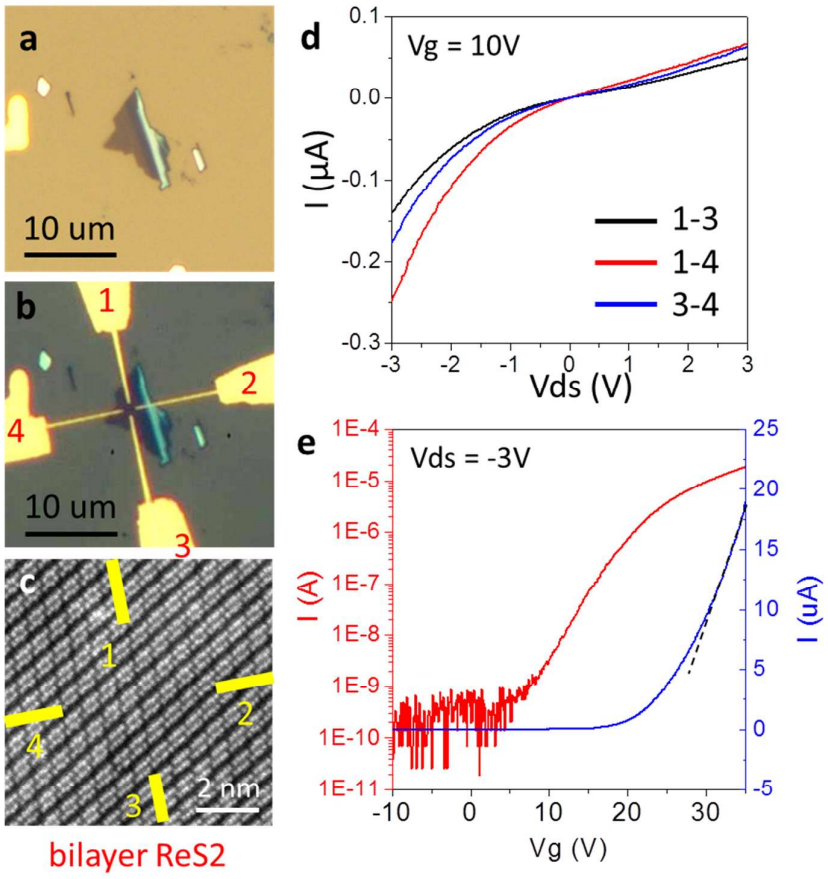

Supplementary Figure S5. The optical microscope images of (a) an exfoliated ReS_2 flake on SiO_2/Si substrate and (b) Four contacts are deposited on the single layer region. (c) An ADF image of the single layer ReS_2. (d) The direction-dependent I-V characteristics with applied back gate voltage Vg=10V. The two-terminal conductance along different direction G_{14}=0.28 μS, G_{34}=0.122 μS and G_{13}=0.112 μS for Vds=-3V and Vg=10V. (e) The transfer characteristic with drain-source bias of -3V between probes 1-4. The field effect mobility is 38.5 cm^2/Vs.

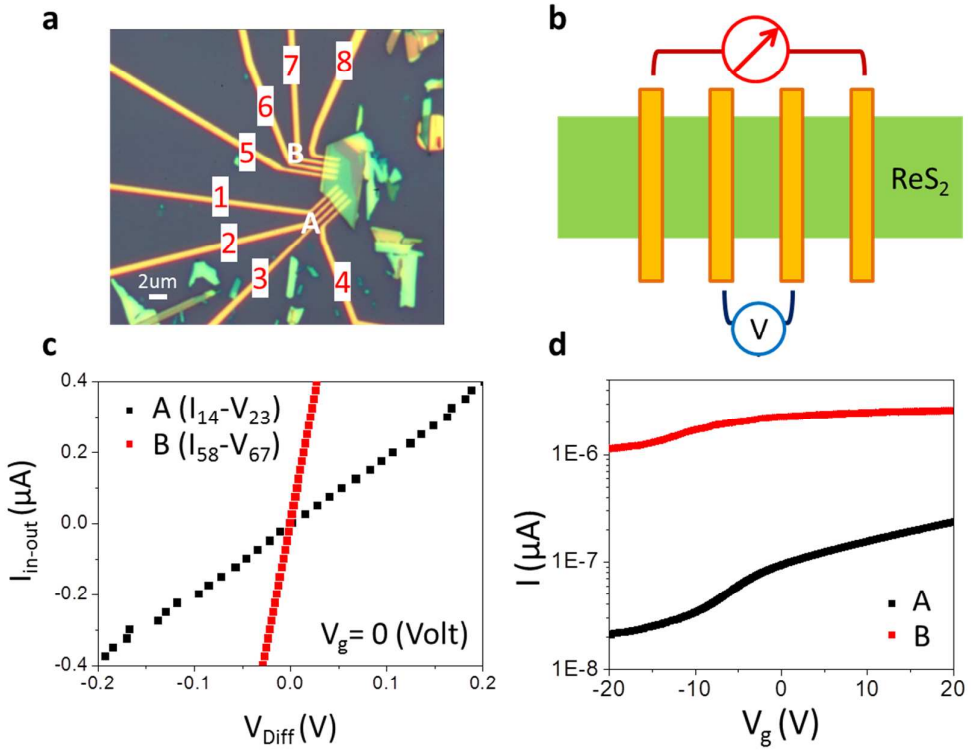

Supplementary Figure S6. (a) An optical image of multilayer ReS_2 FET contacted with 4-terminal contacts along **a** and **b** axes. (b) A schematic of 4-terminal measurement. (c) The 4-terminal I-V characteristic. The device A is measured along the **a** axis, while the device B is measured along the **b** axis. R_A=521.69 kΩ, R_B=69.86 kΩ. (d) The transfer characteristic of device A and B. The field effect mobility is about 4.7 cm^2/Vs along the **b** axis.

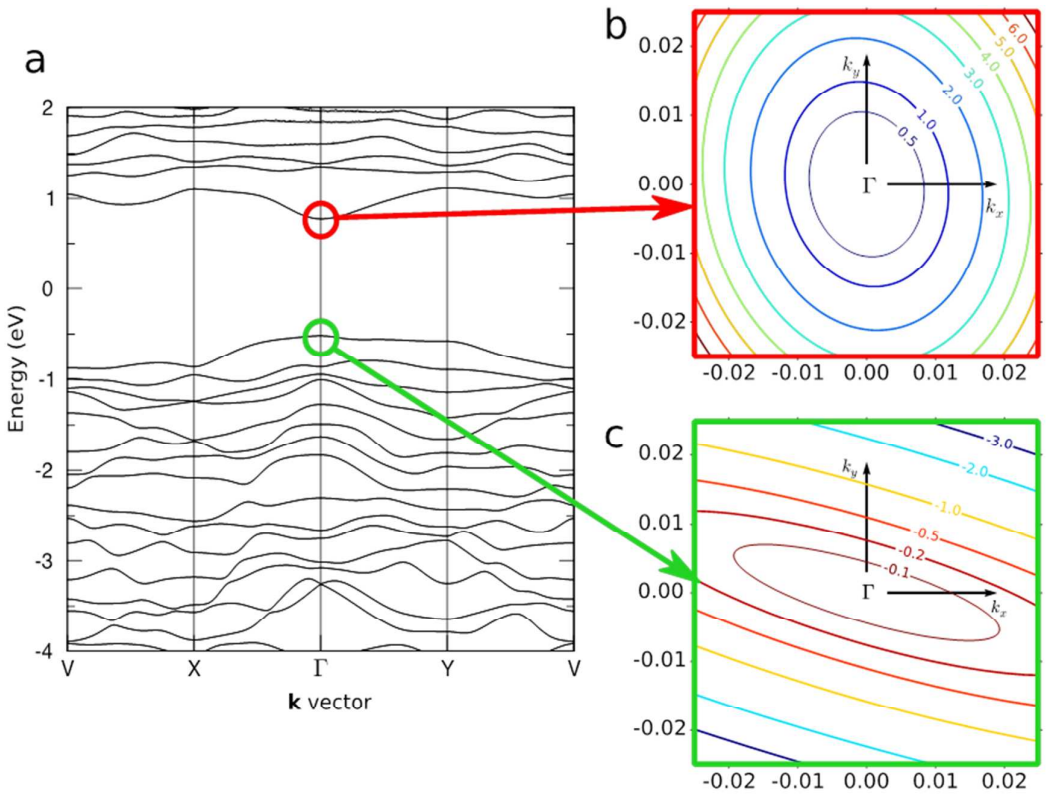

Supplementary Figure S7. (a) The DFT calculated band structure of ReS_2, (b) a contour plot of second order fits of the band dispersion of the conduction band minimum and (c) the valence band maximum. The k_x direction is along the DS chains and we note that the valence band shows significantly stronger anisotropy than the conduction band. The valence band maximum has the shape of a long ridge without a distinct single maximum, making $k \cdot p$ perturbation theory impractical in this case.

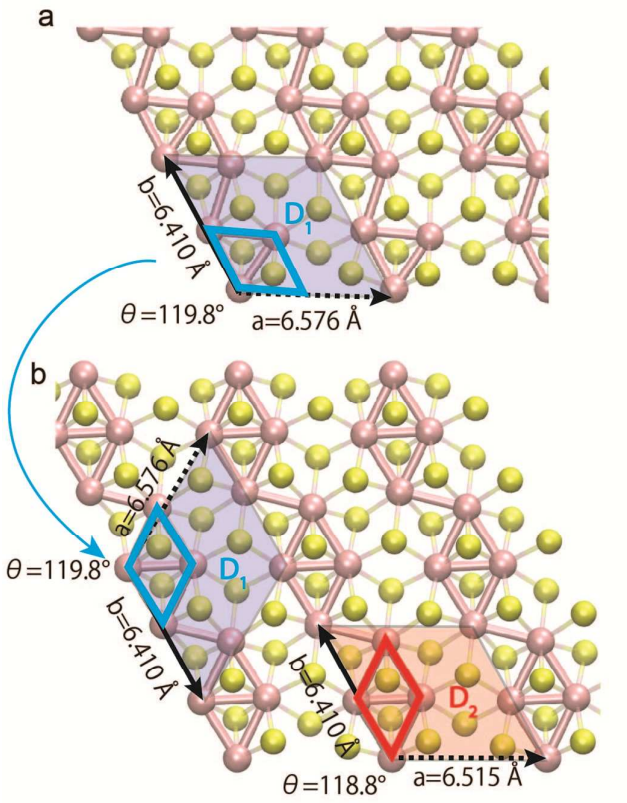

Supplementary Figure S8. (a) Atomic structure of ReS_2 and the illustration of D_1 structure. (b) Atomic structure of ReS_2 and the illustration of D_2 structure. Two nonequivalent choices for **a** lattice vector, depending on the direction of **b** lattice vector.

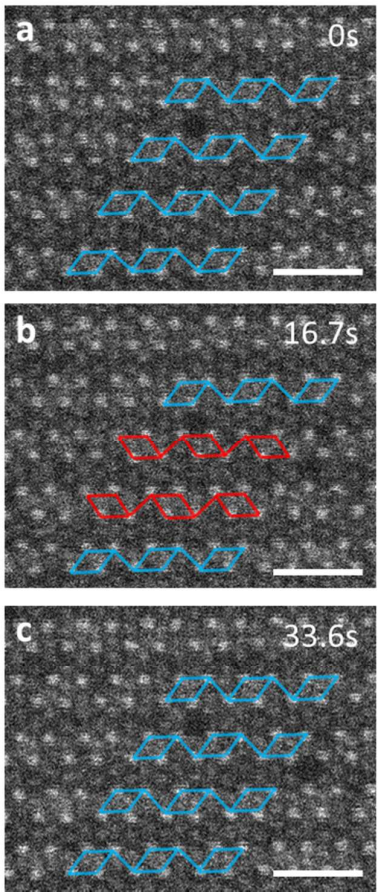

Supplementary Figure S9. (a)-(c) The sequential ADF image of $ReSe_2$ with diamond flip in the direction parallel to the **b**[010] axis. The simultaneous small Re atoms displacement in the third and fourth Re-diamond chains from the top result in the 120°-counterclockwise diamond flip (blue diamond flip to red diamond in (b)). Such diamond flip is reversible and can transform back to original structure (c). See Supplementary movie 2. Scale bar is 1 nm.

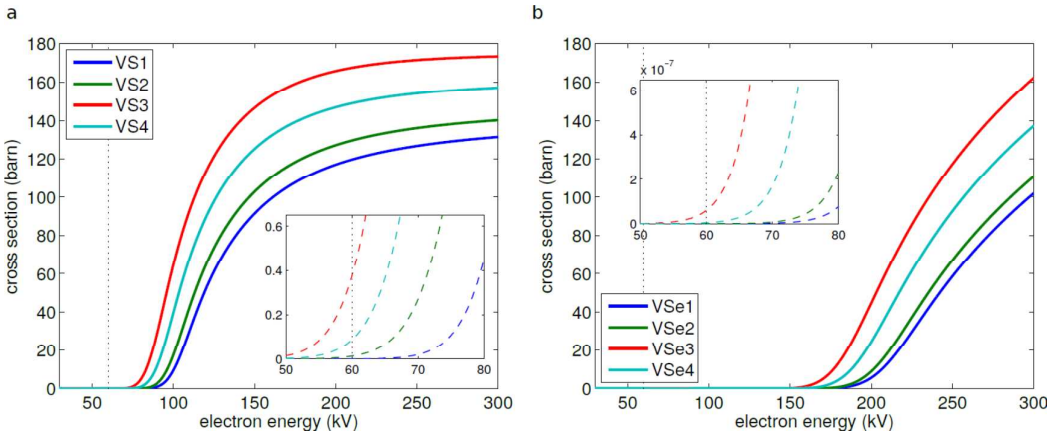

Supplementary Figure S10. Displacement cross sections for the four inequivalent chalcogen vacancies in ReS_2 (a) and $ReSe_2$ (b). Displacement thresholds were evaluated from the unrelaxed vacancies as described in [1] and cross sections calculated using McKinley-Feshbach formalism [2] including the effect of thermal motion of ions [3]. Main panels (solid lines) show room temperature results and the inset (dashed lines) the results at the elevated temperature (500 C) used in the experiments.

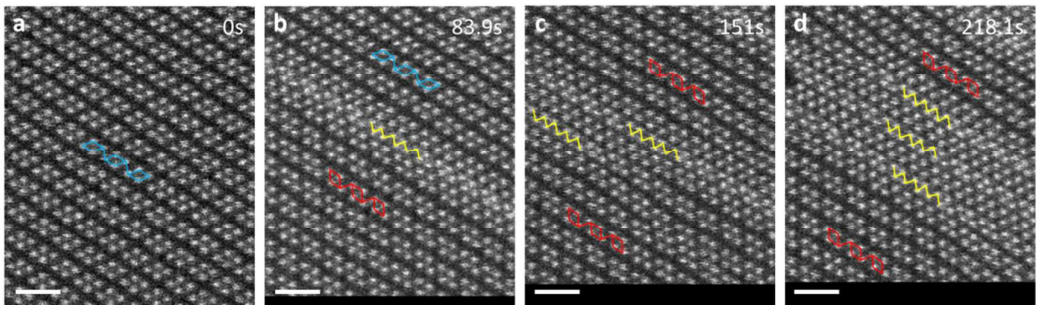

Supplementary Figure S11. (a)-(d) The sequential ADF image of ReS_2, where three Re-diamond chains zip up transformation and form local zigzag chains (yellow lines). The sulfur deficient phase consists of local zigzag chain and sandwiched by diamond chains. See Supplementary Movie 5. Scale bar is 1 nm.

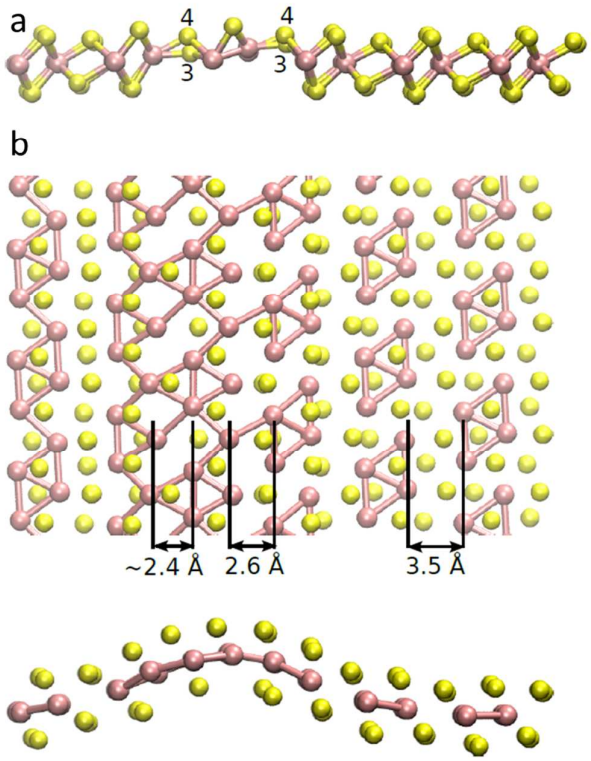

Supplementary Figure S12. (a) The atomic model shown starting configuration consisting of vacancies only in the bottom layer, where one line under the Re-diamonds (position 1 and 2 in Fig. 4) and two lines under the surrounding trenches (position 3 and 4 in Fig. 4). In order to be able to accommodate the squeezing of the lattice, there needs to be vacancies to form the non-stoichiometic phase transformation via diamond chain zipping. We have tried out five different configurations where lines or vacancies were created either in the bottom sulfur layer or positions corresponding to low formation energy. (b) The relaxed structure of zipped-up DS-chains configuration with lowest formation energy, which match with the experimental images as shown in Fig. 5. The distances between the Re columns are in reasonable agreement with the measured. Due to having vacancies on only one side, the structure becomes quite strongly bent.

Reference

[1] Komsa, H.-P.; Kotakoski, J.; Kurasch, S.; Lehtinen, O.; Kaiser, U.; Krasheninnikov, A. V., Two-Dimensional Transition Metal Dichalcogenides under Electron Irradiation: Defect Production and Doping, *Phys. Rev. Lett.* **2012**, *109*, 035503.

[2] McKinley, W. A.; Jr. Feshbach, H., The Coulomb Scattering of Relativistic Electrons by Nuclei, *Phys. Rev.* **1948**, *74*, 1759.
[3] Meyer, J.; Eder, F.; Kurasch, S.; Skakalova, V.; Kotakoski, J.; Park, H. J.; Roth, S.; Chuvilin, A.; Eyhusen, S.; Benner, G. *et al.* Accurate Measurement of Electron Beam Induced Displacement Cross Sections for Single-Layer Graphene. *Phys. Rev. Lett.* **2012**, *108*, 196102.